Miniaturized Tool for Optogenetics Based on an LED and an Optical Fiber Interfaced by a Silicon Housing

M. Schwaerzle, P. Elmlinger, O. Paul, *Member, IEEE*, and P. Ruther, *Member, IEEE*

***Abstract*— This paper reports on the design, simulation, fabrication and characterization of a tool for optogenetic experiments based on a light emitting diode (LED). A minimized silicon (Si) interface houses the LED and aligns it to an optical fiber. With a Si housing size of 550×500×380 µm³ and an electrical interconnection of the LED by a highly flexible polyimide (PI) ribbon cable is the system very variable. PI cables and Si housings are fabricated using established microsystem technologies. A 270×220×50 µm³ bare LED chip is flip-chip-bonded onto the PI cable. The Si housing is adhesively attached to the PI cable, thereby hosting the LED in a recess. An opposite recess guides the optical fiber with a diameter of 125 µm. An aperture in-between restricts the emitted LED light to the fiber core. The optical fiber is adhesively fixed into the Si housing recess. An optical output intensity at the fiber end facet of 1.71 mW/mm² was achieved at a duty cycle of 10 % and a driving current of 30 mA.**

I. Introduction

Neuroscientific research deals with the function and dysfunctions of the brain by analyzing the neuronal circuitry. To achieve this goal, the interaction with the intracerebral signal flow at the neuronal level is indispensable. There is not only the need to observe neuronal communication, but stimulation or inhibition of neuronal activity is required as well. A wide variety of tools for the electrical observation is available. These range from simple wire electrodes [1] via micromachined electrode arrays [2] to CMOS-integrated high-density electrode arrays [3]. Although the electrical stimulation of neural tissue is possible, it bears the risk of cell damage due to high current densities [4] as well as unintended stimulation of neighboring neurons.

Optogenetics has become a much appreciated tool for the stimulation and inhibition of neuronal activity [5], offering in addition cell type specificity, if appropriately designed. These exceptional capabilities increase the number of options for carrying experiments and thus progressing in the understanding of the brain. The number of so-called optrodes, i.e., miniaturized probes for optogenetic experiments, has grown steadily. The common solution of using an optical fiber connected to an external light source [6-8] suffers from the relative stiffness of optical fibers and the unavailability of rotary optical joints for a multitude of fibers. Integrated solutions have circumvented this problem by bringing the light source close to the brain, e.g. by integrating bare laser diode chips on a relatively bulky probe base [9] or inserting an LED on a flexible substrate into the brain tissue [10], at the risk of considerable local heat dissipation.

In the present paper we try to circumvent these drawbacks by a solution, where a short optical fiber is combined with an LED and PI cable in an assembly offering the advantages of a low height, small weight, and high mechanical flexibility of the purely electrical interconnection to the external instrumentation. It can be implanted using dedicated insertion vehicles as available for intracortical microprobes [13]. In combination with recording microelectrodes, the new tool lends itself in principle for acute to chronic optogenetic experiments.

II. System Approach

A. Probe Design

Fig. 1(a) shows a schematic of the probe concept with a polyimide (PI) ribbon cable used as the electrical interface to a light emitting diode (LED), a silicon housing, and an optical glass fiber used to direct light into the neural tissue. The Si interface serves as the housing of the LED and

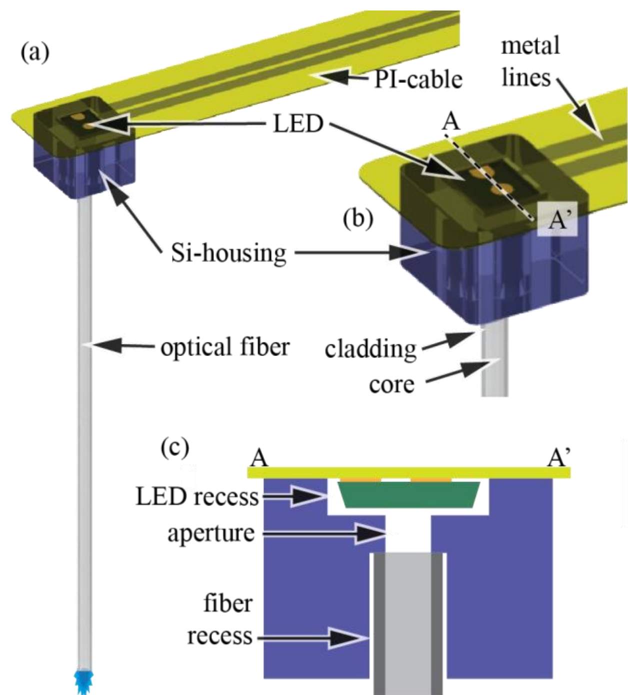

Figure 1. (a) Schematic of the optical tool with LED, highly flexible PI ribbon cable, Si housing, and optical glass fiber; (b) close-up view indicating metal lines in the PI cable for electrically interconnecting the LED; (c) cross-section through a tool along A-A' as indicated in (b) illustrating the relative position of fiber and LED. The Si housing with minimal dimensions of 550×500×380 µm³ acts as the mechanical link and alignment structure between LED and optical fiber.

This work was supported by BrainLinks-BrainTools Cluster of Excellence funded by the German Research Foundation (DGF, grant number EXC 1086).

M. Schwaerzle, P. Elmlinger, O. Paul, and P. Ruther are with the Department of Microsystems Engineering (IMTEK), Albert-Ludwigs-University of Freiburg, 79110 Freiburg, Germany (phone: +49-761-203-67913; fax: +49-761-203-7192; e-mail: michael.schwaerzle@imtek.uni-freiburg.de).

978-1-4244-7929-0/14/$26.00 ©2014 IEEE

guarantees the orthogonal alignment of the optical fiber with respect to the LED.

The LED is mounted directly on the PI-based ribbon cable {Fig. 1(b, c)} comprising two leads and contact pads for electrically interfacing with the LED. The Si housing is used as a mechanical protection of the LED as well as an alignment structure and aperture of the optical fiber. The cross-sectional schematic shown in Fig. 1(c) illustrates the required recesses to host the LED and glass fiber, as well as the through-hole acting as the aperture. The latter channels the light emission from the LED into the fiber core and minimizes the optical power coupled into the fiber cladding.

B. *Simulation*

To verify the system concept of a short glass fiber coupled to a bare LED chip, we simulated the optical components using the ray-tracing tool Zemax (Zemax LLC, Redmond, WA, USA) with respect to the coupling losses and transmitted light intensity. The simulation was done with refractive indices of core, cladding, and surrounding tissue of 1.48, 1.45, and 1.37 [11], respectively. Figs. 2(a) and (b) show a side view of the simulation and the resulting output intensity, respectively. In the side view, the LED is shown at the very left followed by an aperture and an optical glass fiber with core and cladding. As indicated in Fig. 2(a), light mainly couples into the core of the optical fiber. The opening angle of the ray bundle at the right side gives an impression of the illuminated spot at the end of a flat facet. The analysis of the output power at the facet surface {Fig. 2(b)} indicates three regions, i.e. (i) the inner core (green), (ii) the cladding (light blue), and (iii) an outer circle (lighter purple) representing tissue surrounding the fiber. In total, 17.1 % of the input intensity emitted by the LED is transmitted through the fiber and the surrounding tissue. 87.1 % thereof is guided within the core, while 11.1 % are transferred via the cladding. In total 1.8 % is lost via the cladding into the surrounding tissue along the entire fiber length of 5 mm.

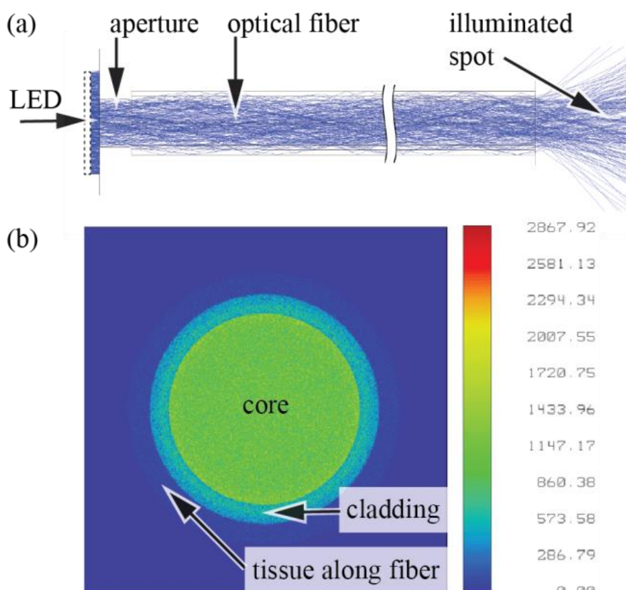

Figure 2. Ray tracing simulation of the system with (a) a side view and (b) the intensity distribution in the output facet. Main components in (a) are the LED on the left, the aperture, and the 5-mm-long optical fiber.

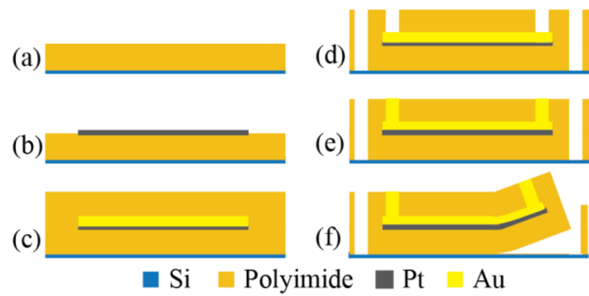

Figure 3. Processing of highly flexible PI-based ribbon cables: (a) Spin-coating of a 5-µm-thick PI layer; (b) deposition and patterning of the Pt metallization using sputtering and lift-off; (c) Au electroplating to increase wire thickness and spin-coating of a second PI layer; (d) pad opening and cable patterning by RIE; (e) thickening of pads by a second Au electroplating step; and (f) cable release.

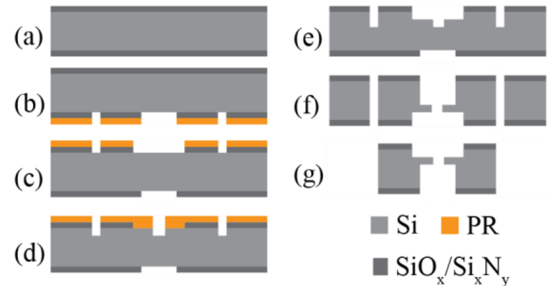

Figure 4. Processing of the Si housing: (a) Deposition of SiO_x/Si_xN_y layer stacks on both wafer sides using PECVD; patterning of (b) rear and (c) front side SiO_x/Si_xN_y masking layers using RIE; (d-f) DRIE steps to define recesses and aperture; and (g) release of Si housing.

C. *Fabrication*

The fabrication of the PI ribbon cable based on Ref. 12 is illustrated in Fig. 3. It applies spin-coating of PI (U-Varnish S, UBE, Tokyo, Japan) to a thickness of 5 µm onto a 4-inch Si handle wafer {Fig. 3(a)}. After curing the PI at 450°C, a 250-nm-thick platinum (Pt) metallization is sputter deposited and structured by lift-off using the AZ 5214E image reversal photoresist {Fig. 3(b)}. The metal tracks and contact pads are thickened in a maskless process by electroplating a 1-µm-thick gold (Au) layer. As shown in Fig. 3(c), a second 5-µm-thick PI layer protects the metal tracks and pads. Both PI layers are patterned to access the contact pads and define the shape of the cable in a single, reactive ion etch (RIE) step using AZ 9260 photo resist as masking layer {Fig. 3(d)}. The contact pads are reinforced by a second Au electroplating step. Individual PI cables are peeled from the substrate using tweezers {Fig. 3(f)}.

The Si housing is manufactured by a three-step deep reactive ion etching (DRIE) process using 380-µm-thick dual side polished Si wafers. The fabrication process summarized in Fig. 4 starts with depositing 4.6-µm-thick, stress-compensated SiO_x/Si_xN_y layer stacks on the wafer front and rear using plasma enhanced chemical vapor deposition (PECVD) {Fig. 4(a)}. This is followed by the patterning of the SiO_x/Si_xN_y layer stacks on the wafer rear using RIE; in a subsequent DRIE step, the respective pattern defines the recess for the optical fiber {Fig. 4(b)}. The masking pattern for the LED recess and outer geometry of the Si housing are then transferred into the front side masking layer using RIE {Fig. 4(c)}. A third photoresist mask is used for the first

DRIE step from the wafer front with an etch depth of 70 µm. It defines the pattern of the aperture inside the Si housing {Fig. 4(d)}. Next, the resist is stripped and a second DRIE step using the patterned SiO_x/Si_xN_y layer stacks as etch mask defines the 70-µm-deep LED recess {Fig. 4(e)}. The same DRIE step extends the aperture to a depth of 140 µm. The final DRIE process from the wafer rear with an etch depth of 240 µm defines the guiding structure of the optical fiber and opens the aperture {Fig. 4(f)}. Again, the initially patterned SiO_x/Si_xN_y layer stacks act as the masking layer during the DRIE steps.

The glass fibers are diced to application specific lengths between 4 and 12 mm using a conventional wafer saw. The fiber alignment and fixation is achieved using trenches diced into a handle wafer with photoresist serving as an adhesive. While the fiber facet on the LED-side is diced or cleaved at 90°, the fiber tip may as well be diced at 45° which is expected to facilitate fiber implantation into neural tissue.

D. *Assembly*

The system assembly is illustrated in Fig. 5. First, a bare LED chip (C460TR2227-S2100, Cree Europe GmbH, Unterschleißheim, Germany) with a size of 270×220×50 µm³ and a center wavelength of 460 nm is flip-chip bonded onto the contact pads of a PI cable using the Fineplacer 96λ from Finetech, Berlin, Germany {Fig. 5(a)}. An appropriate combination of pressure (bond force 1.5 N), ultrasonic energy (300 mW) and temperature (120°C) leads to an Au-Au bond ensuring the electrical as well as mechanical connection between LED and cable. As illustrated in Figs. 5(b) and (c), the Si housing is then attached to the PI cable using a UV-curable adhesive (NOA164, Norland, Cranbury, NJ, USA). Next, a droplet of the adhesive with adapted refractive index is deposited into the Si housing {Fig. 5(d)} in order to ultimately seal the LED cavity. For the fiber alignment, an optical iris is aligned with respect to the Si housing aperture {Fig. 5(e)}. The fiber is inserted into the recess through the fully opened iris {Fig. 5(f)}. This is followed by the application of one more droplet of the NOA164 adhesive {Fig. 5(g)}. Finally, closing the iris and illuminating the assembly with UV light from the side as well as through the optical fiber stabilizes the aligned fiber by curing the adhesive {Fig. 5(h)}.

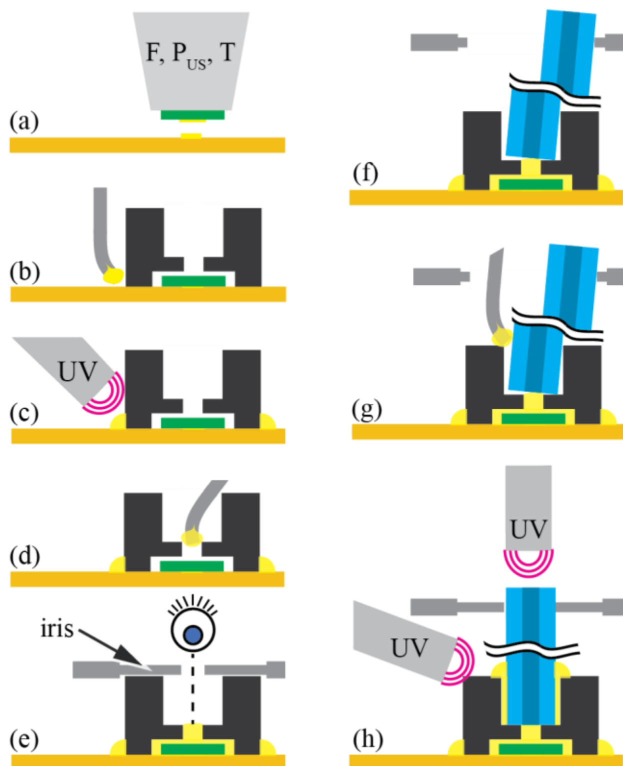

Figure 5. System assembly: (a) Mechanical fixation and electrical interconnection between bare LED chip and PI-cable using a flip-chip bonder; (b) positioning and (c) attachment of Si housing using UV curable adhesive; (d) additional adhesive applied to fill LED recess; (e) alignment of closed iris relative to aperture; (f-g) fiber insertion, alignment and fixation by (f) applying adhesive, (g) closing optical iris, and (h) curing adhesive by UV exposure.

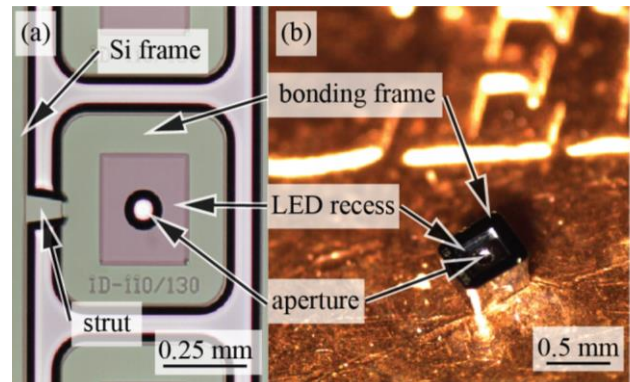

Figure 6. (a) Processed Si housing at wafer level with an aperture of 110 µm and fiber recess with a diameter of 130 µm. (b) Released Si housing on Euro-cent coin.

III. RESULTS

Fig. 6(a) shows the front face of a Si housing realized using the fabrication process in Fig. 4. The housings with minimal outer dimensions down to 550×500 µm² are suspended in the fabrication wafer by thin Si struts. The Si housings are realized with different outer dimensions as well as recess and aperture sizes in order to extract optimally suited geometries. Silicon housings are released from the wafer by breaking their struts {Fig. 6(b)}.

The electroplating of the metal lines on the PI-cable reduces the resistance from 172.5±8.3 Ω to 11.7±0.8 Ω for a

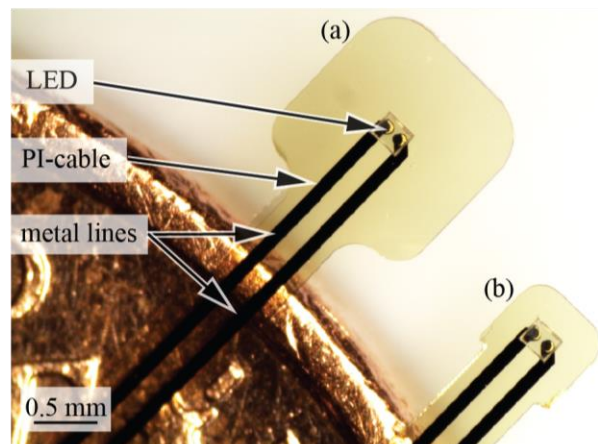

Figure 7. Photograph of LEDs flip-chip-bonded (a) 1950×1950 µm² and (b) 750×700 µm² large PI cable pads before assembly with the Si housing.

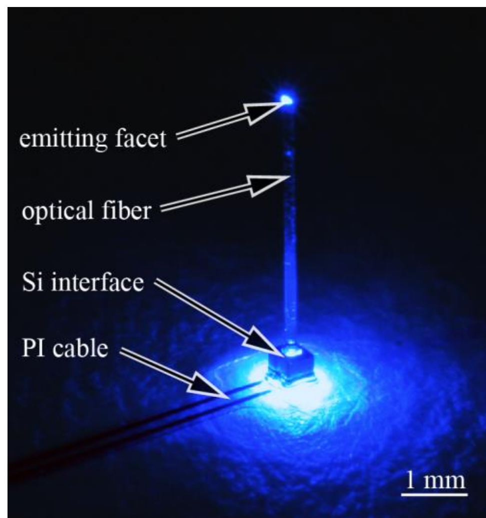

Figure 8. Fully assembled system driven by a current of 20 mA. The individual components (PI cable, SI housing, and optical fiber) are clearly visible. Light coupled from the LED through the SI housing into the fiber is transmitted to the emitting facet of the fiber.

3-cm-long cable. Similarly to the Si housings, the PI cables were designed and processed with a range of dimensions. Fig. 7 shows a photograph of a 1950×1950 µm² and a 750×700 µm² PI cable pad each carrying a flip-chipped LED. The plated Au metal lines buried between the two Pi layers appear in black.

A fully assembled system with PI cable, Si housing, and an optical fiber is shown in Fig. 8. The system is powered with a current of 20 mA. Due to the LED illumination characteristics a considerable fraction (about 50 %) of the light is emitted into the rear direction and thus illuminates the PI cable. A rear reflector, yet to be developed, may improve the efficiency. The light emitted towards the front is partly blocked by the aperture and coupled into the fiber core. At the emitting fiber facet the transmitted light is decoupled and enables the optical stimulation of tissue nearby. Nevertheless, a significant light fraction leaks through adhesive filled gaps.

With the adapted flip-chip bond process we achieved a yield of 89 % for 48 bonded LEDs. Misalignment and assembly variations lead to coupling losses. The transmission was analyzed using an integrating sphere (ISP-50-I-USB, Ocean Optics, Ostfildern, Germany). For this purpose the housing was molded with black epoxy and only the fiber tip was inserted into the sample window of the integrating sphere. Measurements of optical fibers with a core diameter of 105 µm showed output intensities up to 1.03 mW/mm² for the diced fibers and 1.71 mW/mm² for the cleaved fibers with a duty cycle of 10 % at a drive current of 30 mA. According to Ref. 7, this intensity is sufficient for optogenetic applications. The output intensity was found to scale close to linearly with LED current. Simultaneously, we determined the light spectrum emitted by the fiber tip to be centered on 456 nm.

IV. Conclusions

We reported the design, simulation, processing, and assembly of an optical tool with minimal dimensions for optogenetic applications and demonstrated its functionality. The combination of an optical fiber, a miniaturized housing, and a highly flexible PI cable makes the tool suitable for in-vivo experiments. With an output intensity up to 1.71 mW/mm² at a center wavelength of 456 nm the tool lends itself for the optical stimulation of transfected neurons. The small system size allows the nearby implantation of standard wire electrodes [1] and Si micro electrode arrays [2-4] for electrical recording of optically modulated neural activity.

Acknowledgment

The authors gratefully acknowledge Armin Baur, Michael Reichel, and Nico Lehmann for support during the cleanroom fabrication, and Daniel Kopp for the support with the ray tracing simulations.

References

[1] M. A. L. Nicolelis, "Methods for Neural Ensemble Recordings", 2nd ed., *CRC Press*, 2007.
[2] K. D. Wise, A. M. Sodagar, Y. Yao, M. N. Gulari, G. E. Perlin and K. Najafi, "Microelectrodes, microelectronics, and implantable neural microsystems", *Proc. IEEE*, vol. 96, no. 7, pp. 1184-1202, Jul. 2008.
[3] K. Seidl, M. Schwaerzle, I. Ulbert, H.P. Neves, O. Paul, and P. Ruther, "CMOS-based high-density silicon microprobe arrays for electronic depth control in intracortical neural recording-characterization and application", *IEEE J. Microelectromech. Syst.,* vol. 21, no. 6, pp. 1426-1435, Dec. 2012.
[4] A. Butterwick, A. Vankov, P. Huie, Y. Freyvert and D. Palanker, "Tissue damage by pulsed electrical stimulation", *IEEE Trans. Biomed. Eng.*, vol. 54, no. 12, pp. 2261-2267, Dec. 2007.
[5] O. Yizhar, L. E. Fenno, T. L. Davidson, M. Moguri, and K. Deisseroth, "Integrated device for optical stimulation and spatiotemperal electrical recording of neural activity in light-sensitized brain tissue", *Neuron*, vol. 71, pp. 9-34, Jul. 2011.
[6] S. Royer, B.V. Zemelman, M. Barbic, A. Losonczy, G. Buzsáki, and J.C. Magee, "Multi-array silicon probes with integrated optical fibers: light-assisted perturbation and recording of local neural circuits in the behaving animal", *European J. of Neurosci.*, vol. 31, pp. 2279-2291, Mar. 2010.
[7] J. Wang, F. Wagner, D.A. Borton J. Zhang, I. Ozden, R.D. Burwell, A.V. Nurmikko R.V. Wagenen, I. Diester, and K. Deisseroth, "Integrated device for combined optical neuromudulation and electrical recording for chronic in vivo applications", *IEEE J. Neural Eng.,* vol. 9, 016001, 14 pp, Dec. 2011.
[8] B. Rubehn, S.B.E. Wolff, P. Tovote, A. Lüthi, and T. Stieglitz, "A polymer-based neural microimplant for optogenetic applications: design and first in vivo study", *Lab Chip*, vol. 13, pp. 579-588, Jan. 2013.
[9] M. Schwaerzle, K. Seidl, U.T. Schwarz, O. Paul, and P. Ruther, "Ultracompact optrode with integrated laser diode chips and SU-8 waveguides for optogenetic applications", *IEEE MEMS Conf. Proc.*, 2013, pp. 1029-1032.
[10] T.-I. Kim, J.G. McCall, Y.H. Jung, X. Huang, E.R. Siuda, Y. Li, J. Song, Y.M. Song, H.A. Pao, R.-H. Kim, C. Lu, S.D. Lee, I.-S. Song, G. Shin, R. Al-Hasani, S. Kim, M.P. Tan, Y. Huang, F.G. Omenetto, J.A. Rogers, and M.R. Bruchas, "Injectable, cellular-scale optoelectronics with applications for wireless optogenetics", *Science*, vol. 340, pp. 211-216, Apr. 2013.
[11] J. Sun, S.J. Lee, L. Wu, M. Sarntinoranont, and H. Xie, "Refractive index measurement of acute rat brain tissue slices using optical coherence tomography", *Optics Express,* vol. 20, no. 2, pp. 1084-1095, Jan. 2012.
[12] S. Kisban, J. Kenntner, P. Janssen, R.v. Metzen, S. Herwik, U. Bartsch, T. Stieglitz, O. Paul, and P. Ruther, "A novel assembly method for silicon-based neural devices", *IFMBE Conf. Proc.,* 2009, pp. 107-110.
[13] S. Kisban, P. Janssen, S. Herwik, T. Stieglitz, O. Paul, and P. Ruther, "Hybrid microprobes for chronic implantation in the cerebral cortex", *IEEE EMBC Conf. Proc.,* 2008, pp. 2016-2019.